Structure−Activity Relationship Studies of a Series of Novel δ-Lactam-Based Histone Deacetylase Inhibitors

Hwan Mook Kim,[†] Dong-Kyu Ryu,[†] Yongseok Choi,[‡] Bum Woo Park,[†] Kiho Lee,[†] Sang Bae Han,[†] Chang-Woo Lee,[†] Moo-Rim Kang,[†] Jong Soon Kang,[†] Shanthaveerappa K. Boovanahalli,[†] Song-Kyu Park,*[,†] Jung Whan Han,[§] Tae-Gyu Chun,[||,⊥] Hee-Yoon Lee,[||] Ky-Youb Nam,[#] Eun Hyun Choi,[⊥] and Gyoonhee Han*[,⊥]

Bioevaluation Center, KRIBB, Daejeon 305-806, Korea, School of Life Sciences and Biotechnology, Korea University, Seoul 136-701 Korea, College of Pharmacy, Sung Kyun Kwan University, Suwon, Gyeonggi-do 440-746, Korea, Department of Chemistry, KAIST, Daejeon 305-701, Korea, Research Institute Bioinformatics and Molecular Design (BMD), Yonsei Engineering Research Complex, Seodaemun-gu, Seoul 120-740, Korea, and Department of Biotechnology, Yonsei University, Seodaemun-gu, Seoul 120-740, Korea

Received December 1, 2006

We synthesized a series of δ-lactam-based HDAC inhibitors that were identified with various degrees of anti-inflammatory and cell growth inhibitory activities. Compounds possessing significant HDAC inhibitory activity exhibited both anti-inflammatory and cell growth inhibitory activities as well as significant tumor growth inhibition in the *in vivo* tumor xenograft experiments. Besides, these compounds demonstrated anti-inflammatory properties *in vitro* via suppression of the production of the proinflammatory cytokine TNF-α and nitric oxide by LPS-stimulated RAW264.7 cells.

Introduction

The first connection between inflammation and cancer was made much earlier by Rudolf Virchow when he discovered leucocytes in neoplastic tissues and linked tumor with inflammation.[1] Since then, a substantial body of evidence has been published to support the conclusion that chronic inflammation represents a key risk factor for cancer and even as a means to prognose/diagnose cancer at the onset of the disease.[2] In addition, recent data have expanded the concept that inflammation is a critical component of tumor progression. The longer the inflammation persists, the higher the risk of associated carcinogenesis.[3] Therefore, new strategies for the prevention and treatment of tumors associated with inflammatory diseases would open new therapeutic avenues.

Histone deacetylases (HDACs[a]) play an important role in gene transcription. Many recent studies show that inhibition of HDACs elicits anticancer effects in several types of tumor cells by inhibition of cell growth and induction of cell differentiation and this has led to the development of specific inhibitors for cancer chemotherapy. In this context, several programs for the development of HDAC inhibitors as an anticancer drug have been initiated, and currently, several compounds are in both preclinical development and clinical trials.[4] HDAC inhibitors such as suberoylanilide hydroxamic acid (SAHA, **1**) and trichostatin A (TSA, **2**), the class of hydroxamic acid-containing hybrid polar molecules, possess antitumor activity as well as anti-inflammatory properties (Figure 1).[5] The anti-inflammatory properties of SAHA have been demonstrated via *in vitro* and *in vivo* suppression of proinflammatory cytokine tumor necrosis factor (TNF-α) as well as inhibition of *in vitro* production of cytokine-induced nitric oxide (NO).[5a] Based on these findings, we hypothesized that the dual anti-inflammatory and antiproliferative activity of HDAC inhibitors is in part attributable to the potent HDAC inhibitory activity. These key findings prompted us to investigate a series of potent HDAC inhibitors for their potential to exhibit anti-inflammatory and antiproliferative activities.

In our search for novel HDAC inhibitors, we recently disclosed a series of δ-lactam-based HDAC inhibitors[6] and we identified a lead compound (**3**) in this series, which showed significant HDAC inhibitory activity comparable to SAHA. Based on this lead molecule, we performed a closely related structural activity relationship (SAR) study and then generated a new series of potent δ-lactam-based HDAC inhibitors, which were evaluated for their anti-inflammatory and antiproliferative activities. These studies were culminated in the identification of a series of potent δ-lactam-based HDAC inhibitors, which demonstrated significant inhibitions of HDAC activity as well as anti-inflammatory and cell growth inhibitory activities. Herein, we report our findings derived from a systematic evaluation of correlation of HDAC inhibition to anti-inflammatory and cell growth inhibitory activities of a new series of novel δ-lactam-based HDAC inhibitors.

Chemistry

The synthesis of δ-lactam analogues **13**−**15** and **21** was accomplished according to the synthetic protocols as illustrated in Schemes 1 and 2.[6] As shown in Scheme 1, reaction of 4-bromo-1-butene with the appropriate amines **4** yielded the corresponding alkylated secondary amines **5**. EDC-mediated coupling of these amines **5** with the appropriate acids **6** afforded the respective intermediates **7**−**9** in good yields. Further cyclization was achieved under mild conditions using catalytic 2−3 mol % of Grubb's catalyst (I) in high yields. The resulting ester derivatives **10**−**12** were then reacted with $KONH_2$ to obtain the desired hydroxamides **13**−**15**. Following a similar sequence of reactions, commercially available 2, 4-dimethoxy

* To whom correspondence should be addressed. Tel.: +82-42-860-4689 (S.-K.P.); +82-2-2123-2882 (G.H.). Fax: +82-42-860-4605 (S.-K.P.); +82-2-3362-7265 (G.H.). E-mail: spark123@kribb.re.kr (S.-K.P.); gyoonhee@yonsei.ac.kr (G.H.).

† Bioevaluation Center, KRIBB.

‡ Korea University.

§ Sung Kyun Kwan University.

|| Department of Chemistry, KAIST.

⊥ Yonsei University.

Research Institute Bioinformatics and Molecular Design (BMD).

[a] Abbreviations: HDAC, histone deacetylase; SAHA, suberoylanilide hydroxamic acid; TSA, trichostatin A; TNF-α, tumor necrosis factor α; NO, nitric oxide; CAP, hydrophobic aromatic groups; DMB, dimethoxybenzyl; EDC, 1-ethyl-3-(3-dimethylaminopropyl)-dicarboximide hydrochloride.

10.1021/jm0613828 CCC: $37.00
Published on Web 05/04/2007

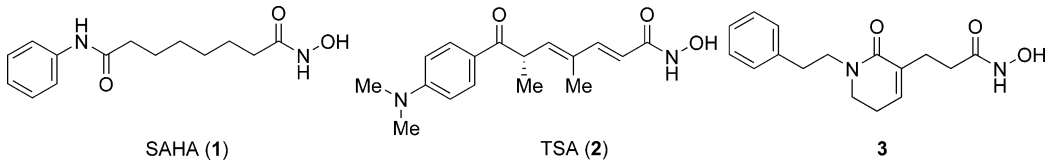

Figure 1. Chemical structure of SAHA and TSA.

Scheme 1[a]

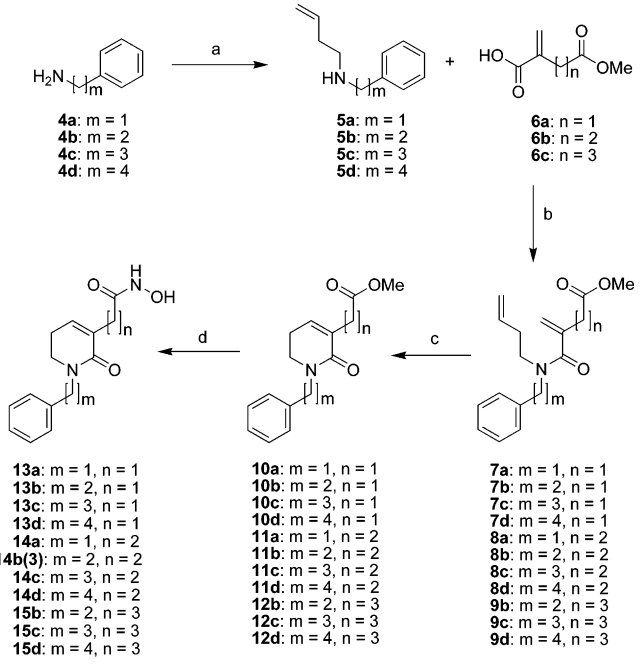

[a] Reagents and conditions: (a) 4-bromo-1-butene, hunig's base, reflux; (b) EDCI, DMAP, CH_2Cl_2, rt; (c) Grubb's catalyst (I), rt; (d) $KONH_2$, MeOH, 0 °C to rt.

Scheme 2[a]

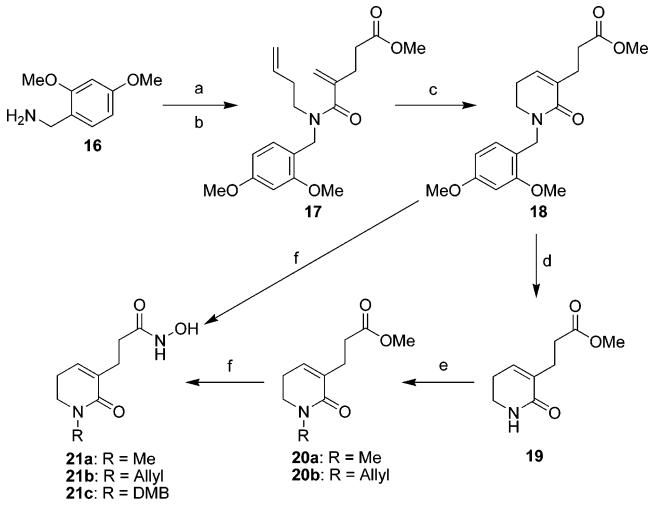

[a] Reagents and conditions: (a) 4-bromo-1-butene, hunig's base, reflux; (b) **6b**, EDCI, DMAP, CH_2Cl_2, rt; (c) Grubb's catalyst (I), rt; (d) TFA, triethylsilane, reflux; (e) NaHMDS, −78 °C, 0.5 h, then Me_2SO_4 for **20a**, allyl bromide for **20b**, −78 °C to 0 °C; (f) $KONH_2$, MeOH, 0 °C to rt.

benzylamine **16** furnished the required intermediate **18**, which was subsequently converted directly to the required hydroxamide **21c** under the usual reaction conditions described for the previous hydroxamides. Displacement of the 2,4-dimethoxy benzyl moiety in compound **18** was achieved under reflux conditions in trifluoroacetic acid to obtain intermediate **19** in good yield, which underwent alkylation to provide alkylated analogues **20a**,**b**. Subsequent reaction of **20a**,**b** with $KONH_2$ afforded the corresponding hydroxamides **21a**,**b** (Scheme 2).

Table 1. In Vitro Inhibition of the Activity of HDAC Enzyme and the Production of TNF-α and NO by SAHA and δ-Lactam Analogues **13**−**15** and **21**[a]

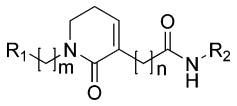

					IC$_{50}$ (μM)		
cmpd	m	n	R_1	R_2	HDAC[b]	TNF-α[c]	NO[c]
13a	1	1	Ph	OH	NA[e]	NA	NA
13b	2	1	Ph	OH	NA	NA	NA
13c	3	1	Ph	OH	NA	NA	NA
13d	4	1	Ph	OH	NA	NA	NA
14a	1	2	Ph	OH	0.67	3.31	3.09
14b (3)	2	2	Ph	OH	0.35	1.90	4.27
14c	3	2	Ph	OH	0.27	1.10	2.71
14d	4	2	Ph	OH	0.13	1.30	1.80
15b	2	3	Ph	OH	NA	NA	NA
15c	3	3	Ph	OH	3.21	NA	6.57
15d	4	3	Ph	OH	NA	NA	6.74
21a	1	2	H	OH	NA	NA	NA
21b	1	2	−CH=CH$_2$	OH	4.27	10.96	NA
21c	1	2	DMPh[d]	OH	0.50	5.06	5.20
SAHA					0.11	0.76	1.88

[a] Values are the means of a minimum of three experiments. [b] HDAC enzyme obtained from HeLa cell lysate. [c] For NO and TNF-α assays, inhibitors were treated in RAW264.7 cells with the range between 0.1 μM and 10 μM. IC$_{50}$ values were calculated to evaluate their ability for suppressing the production of NO and TNF-α. [d] DMPh = 2,4-dimethoxy phenyl. [e] NA = IC$_{50}$ values are higher than 10 μM.

Results and Discussion

Compounds **13**−**15** and **21** were assayed for their HDAC inhibitory activity and anti-inflammatory activity, and the results are tabulated as IC$_{50}$ values in Table 1. SAHA, a known HDAC inhibitor and antitumor agent, was used as a reference compound for comparison. The partially purified HDAC enzyme was obtained from HeLa cell lysate for measuring enzyme inhibitory activity. A potent proinflammatory cytokine TNF-α and a well-known proinflammatory key mediator NO, which play an important role in inflammation, were used as indicators to assess the anti-inflammatory activity of HDAC inhibitors.

HDAC inhibitors SAHA (**1**) and TSA (**2**) and most of their analogues have an aliphatic chain between the hydroxamic acid (zinc binder) and the hydrophobic aromatic groups (CAP group). The alkyl chain of SAHA inserts into the tubular hydrophobic pocket, and the hydroxamic acid group serves as a bidentate chelator of the catalytic Zn^{2+} ion bound in the enzyme active site.[7] The zinc binder and cap groups of the compound **3** were attached through a δ-lactam ring, which mimic the hydrophobic tail group and the aliphatic chain of SAHA, and therefore, this compound also should bind to the hydrophobic cavity in a similar fashion as SAHA. Compound **3** showed potent HDAC inhibition, with an IC$_{50}$ value of 0.35 μM, and was chosen as a starting template for the generation of a new series of δ-lactam analogues. Because we hypothesized that the placement of an appropriate spacer between the zinc binder and cap group

would modulate the HDAC inhibitory activity, our SAR was focused on the following modifications: (i) the variation of the chain length between the zinc binder and the cap group by retaining the δ-lactam ring, (ii) altering the cap group with different alkyl and aromatic groups, and (iii) replacement of the hydroxamic acid group with an *o*-aminoanilide moiety.

To assess the effect of the chain length, we prepared various hydroxamic acid derivatives with varying chain lengths between the zinc binder and the cap group, which resulted in the analogues **13**−**15** having 1−4 carbon units between the cap group and the δ-lactam ring, in addition to 1−3 carbon units between the δ-lactam ring and the hydroxamic acid moiety. We first examined analogues **13a**−**d** having 1−4 carbon units between the cap group and the δ-lactam ring, in addition to a methylene bridge between the δ-lactam ring and the zinc binder group for their ability to inhibit HDAC enzyme, but all of these analogues were found to be inactive. We then investigated the effect of elongation of the alkyl linker by two carbon units between the δ-lactam ring and the zinc binder group by maintaining 1−4 carbon units between the cap group and the δ-lactam ring. Interestingly, this modification, which is represented by analogues **14a**−**d**, demonstrated appreciably high inhibitory activity as good as SAHA's. Encouraged by these results, we further increased the length of the alkyl linker by three methylene units between δ-lactam ring and zinc binder group, but this led to the complete loss of potency, with the exception of analogue **15c**, which displayed moderate inhibitory activity. From these results it is evident that the potency of δ-lactam analogues is directly related to the alkyl linker between the cap group and the zinc binder group, suggesting that the presence of 3−4 carbon units between the cap group and the δ-lactam ring, in addition to two carbon units between the δ-lactam ring and the zinc binder group is optimal for potency. Having established the optimal chain length for potency, we were interested in exploring the effects of altering the cap group and the zinc binder group to assess whether such modifications could affect potency. Replacements of the phenyl cap group with methyl, allyl, and dimethoxy phenyl was investigated by synthesizing analogues **21a**−**c**. However, only dimethoxy phenyl derivative **21c** showed significant potency, with an IC_{50} value of 0.5 μM, which emphasizes that a phenyl group at this position is optimal for potency.

To examine whether there exists a correlation between HDAC enzyme inhibition and anti-inflammatory activity, these analogues were further assayed for their ability to inhibit the production of TNF-α and NO by RAW264.7 cells. Interestingly, analogues **14a**−**d** and **21c**, possessing significant HDAC inhibitory activity, greatly inhibited the production of both TNF-α and NO, while compounds **15c** and **21b**, with moderate HDAC inhibitory activity, displayed reasonable inhibition of both TNF-α and NO. On the other hand, compounds **13a**−**d**, **15b**, and **21a**, which failed to inhibit HDAC enzyme, were also found to be inactive to inhibit the production of TNF-α and NO, with the exception of analogue **15d**, which inhibited NO production considerably. Thus, only compounds capable of inhibiting HDAC enzyme were able to inhibit the production of TNF-α and NO. These results strongly support our hypothesis that there exists a correlation between HDAC inhibitory activity and anti-inflammatory activity among this class of compounds.

Because it is well documented in the literature that HDAC inhibitors display cell growth inhibitory activity, analogues **14a**−**d** and **21c**, possessing significant HDAC inhibitory activity, were further tested for their antiproliferative effect using a panel of cancer cell lines, which consisted of HCT-15, LOX-IMVI, PC-3, ACHN, MDA-MB-231, and NCI-H23 cells. Cell growth inhibition of the tested analogues was measured by SRB assay,[8] and the GI_{50} values obtained for the types of tumor cell lines are summarized in Table 2. High cell growth inhibitory potency against the entire cell types was observed with the reference drug SAHA. Analogues **14c**,**d**, the most potent HDAC inhibitors among the series, demonstrated significant antiproliferative activity on all of the cell types examined, with the exception of the inactivity of **14d** on the LOX-IMVI cell line. Whereas compounds **14b** and **21c** were inactive on the NCI-H23 cell line and displayed considerable activity on all of the remaining cell lines, compound **14a** exhibited a considerable growth inhibitory activity only on MDA-MB-231 cells. Thus, overall tumor cell growth inhibitory activities of these analogues are related to their HDAC inhibitory activities.

Table 2. Cell Growth Inhibitory Activities of Analogues **14a**−**d** and **21c**[a]

		growth inhibition[b] (μM)					
cell line	tissue	**14a**	**14b**	**14c**	**14d**	**21c**	SAHA
HCT-15	colon	NA[c]	8.16	4.99	5.37	7.98	0.82
LOX-IMVI	melanoma	NA	5.84	3.34	NA	6.63	1.39
PC-3	prostate	NA	8.58	5.04	1.32	4.55	0.89
ACHN	kidney	NA	7.76	1.17	2.50	9.58	0.73
MDA-MB-231	breast	4.26	1.62	0.50	1.50	2.67	0.66
NCI-H23	lung	NA	NA	3.79	5.14	NA	0.92

[a] Values are the means of a minimum of three experiments. [b] Growth inhibition was measured by SRB (sulforhodamine B) assay. [c] NA = not active.

Table 3. Inhibition of the Growth of the MDA-MB-231 Human Breast Xenograft by Compound **14d** and SAHA[a]

	i.p.[b]	
cmpd	dose (mg/kg)	30
14d	inhibition (%)	51[c]
SAHA	inhibition (%)	39[d]

[a] Nude mice (six per group) were treated. [b] **14d** and SAHA were administered (i.p.) after the size of tumors reached to 50−60 mm^3. [c] $P < 0.001$. [d] $P < 0.01$.

The most promising inhibitor **14d** was selected to be further evaluated for *in vivo* tumor growth inhibitory activity, and the results are summarized in Table 3. In this model, compound **14d** and SAHA were administered daily (i.p., 30 mg/kg) to nude mice after the sizes of MDA-MB-231 human breast xenografts reached to 50−60 mm^3. Compound **14d** and SAHA caused 51% and 39% inhibition of tumor growth, respectively, compared to the group without treatment of HDAC inhibitors. Thus, both compound **14d** and SAHA displayed antitumor growth activities, and **14d** seemed to be better than SAHA in terms of inhibiting the growth of tumor.

To understand the binding mode of these inhibitors, we examined a docking model of human homology HDAC-1 model based on the crystal structure of a bacterial HDAC homologue (HDLP, PDB code 1C3R) and docked compounds **14d** within the site using the program InsightII/Discover (Figure 2).[9] The complex binding model for the analogs were carried out with the Discover program.[10] The δ-lactam ring of **14d** passes through a narrow channel in the binding pocket, which is formed by two aromatic side chains of Phe-142 and Phe-197. The aliphatic chain between the hydroxamate and the δ-lactam ring of **14d** was bound in the tubular hydrophobic pocket, and the hydroxamic acid moiety of **14d** chelates to the catalytic Zn^{2+} ion bound in the active site. The docking data suggest that the chain length between the zinc binder group and the δ-lactam ring is quite important to form the flexible conformation in the binding pocket and that the carbonyl in the δ-lactam ring forms

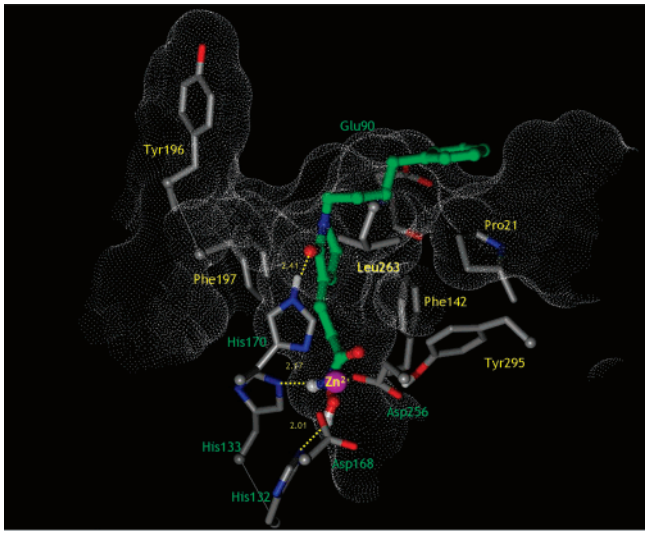

Figure 2. Docked orientations for compound **14d** bound to the HDAC1 catalytic core.

the weak hydrogen bond (2.41 Å) with the side chain of His-170. Furthermore, a longer chain length between the δ-lactam and the phenyl group and the phenyl hydrophobic CAP group give the extra stabilization energy by hydrophobic interaction with Pro-21, Phe-142, and Leu-263.

A series of novel δ-lactam-based HDAC inhibitors possessing both anti-inflammatory and antiproliferative activities were identified through a systematic exploration of SAR studies of a previously reported δ-lactam analogue. The potencies of these δ-lactam analogues are related to the chain length between the CAP group and the zinc binder group, with 3−4 carbon units between the cap group and the δ-lactam ring, in addition to two carbon units optimal for potency between the δ-lactam ring and the zinc binder group, which was also further confirmed by docking studies. The anti-inflammatory properties of these inhibitors were strongly dependent on their HDAC inhibitory potency. Only compounds possessing significant HDAC inhibitory activity demonstrated potent anti-inflammatory properties. Among them, compounds **14c** and **14d** emerged as the most promising HDAC inhibitors, which also demonstrated significant cell growth inhibitory activity against a panel of cell lines. Moreover, compound **14d** showed the considerable extent of tumor growth inhibition in the in vivo tumor xenograft experiment. Besides, these analogues also exhibited anti-inflammatory properties via the potent in vitro and in vivo inhibition of cytokine TNF-α and in vitro inhibition of LPS-induced NO. In summary, these results revealed a correlation between HDAC inhibition and anti-inflammatory and cell growth inhibitory activities of this class of δ-lactam analogues, and further investigation is warranted to establish the mechanism of inhibitory activity. This represents the first report aimed at the identification of a series of HDAC inhibitors possessing anti-inflammatory and antiproliferative properties.

Experimental Section

General. All chemicals were obtained from commercial suppliers and used without further purification. Flash column chromatography was performed with silica (Merck EM9385, 230−400 mesh). ^{1}H and ^{13}C NMR spectra were recorded at 300 and at 75 MHz, respectively. Proton and carbon chemical shifts are expressed in ppm relative to internal tetramethylsilane; coupling constants (J) are expressed in Hertz. Cells were obtained from R&D Systems, Minneapolis, MN. Products from all reactions were purified to a minimum purity of 96%, as determined by reversed phase HPLC (see Supporting Information).

General Procedures for 7−9. Compound **6a**, **6b**, or **6c** (1.2 equiv) was dissolved in methylene chloride and then **5a** in methylene chloride was added via cannular at room temperature under an Ar atmosphere. EDC (1.3 equiv) and DMAP (0.3 equiv) were added, and the mixture was stirred for 8 h at room temperature. The mixture was diluted with ethyl acetate and washed with 5% HCl, satd $NaHCO_3$ solution, and brine, and the organic layer was dried over anhydrous $MgSO_4$. The desired compound (**9**−**11**) was obtained by flash chromatography.

3-(Benzyl-but-3-enyl-carbamoyl)-but-3-enoic Acid Methyl Ester (7a). Compound **5a** (248 mg, 1.53 mmol) was used and **7a** (170 mg, 38%, oil) was obtained by flash chromatography (ethyl acetate/hexanes, 1/1). ^{1}H NMR ($CDCl_3$) δ 7.29 (d, J = 6.9 Hz, 2H), 7.22 (t, J = 6.9 Hz, 3H), 5.69 (br t, 1H), 5.23 (s, 2H), 5.04 (s, 1H), 4.97 (d, J = 9.3 Hz, 1H), 4.71 (d, J = 16.9 Hz, 2H), 3.61 (s, 3H), 3.42 (s, 4H), 2.30 (q, J = 7.2 Hz, 2H); ESI (m/z) 310.5 (MNa^+).

General Procedures for 10−12. Compound **7**, **8**, or **9** was dissolved in methylene chloride (0.01 M), and the mixture was gassed by Ar bubbling for 30 min. After Grubb's catalyst (Type I, 0.02 equiv) was added, the reaction mixture was stirred for 12 h in the dark. The mixture was concentrated in vacuo, and the desired compound (**10**−**12**) was obtained by flash chromatography.

(1-Benzyl-2-oxo-1,2,5,6-tetrahydro-pyridin-3-yl)-acetic Acid Methyl Ester (10a). Compound **7a** (77 mg, 0.26 mmol) was used, and **10a** (50 mg, 74%, oil) was obtained by flash chromatography (ethyl acetate/hexanes, 1/2). ^{1}H NMR ($CDCl_3$) δ 7.30−7.23 (m, 5H), 6.42 (t, J = 4.2 Hz, 1H), 4.61 (s, 2H), 3.69 (s, 3H), 3.32 (t, J = 7.2 Hz, 4H), 2.32 (dd, J = 6.9 Hz, 2H); ^{13}C NMR ($CDCl_3$) δ 171.96, 164.46, 137.34, 136.80, 129.34, 128.55, 127.90, 127.32, 51.91, 50.02, 44.68, 36.38, 23.92; ESI (m/z) 282.4 (MNa^+).

General Procedures for 13−15. Compound **10**, **11**, or **12** was dissolved in methanol (0.5 M solution) and then NH_2OK (1.7 M suspension in methanol, 5.0 equiv) was added at 0 °C. The mixture was stirred for 20 h at room temperature. 10% HCl was added to pH 2−3, and the mixture was concentrated in vacuo. White solid was removed on filter with eluting of methanol/chloroform (1/9). The desired compound (**13**−**15**) was obtained by flash chromatography.

2-(1-Benzyl-2-oxo-1,2,5,6-tetrahydro-pyridin-3-yl)-*N*-hydroxy-acetamide (13a). Compound **10a** (17 mg, 0.07 mmol) was used and **13a** (10 mg, 55%, oil) was obtained by flash chromatography (methanol/chloroform, 1/19). ^{1}H NMR ($CDCl_3$) δ 7.34−7.22 (m, 5H), 6.58 (t, J = 4.5 Hz, 1H), 4.60 (s, 2H) 3.39−3.30 (m, 3H) 3.20 (s, 2H), 2.39−2.30 (m, 2H); ^{13}C NMR ($CDCl_3$) δ 168.44, 165.53, 138.56, 136.73, 128.77, 128.02, 127.88, 127.68, 50.33, 44.81, 36.63, 23.86; ESI (m/z) 283.4 (MNa^+); HRMS (m/z, MH^+) calcd for $C_{14}H_{17}N_2O_3$, 261.1234; found, 261.1226.

4-[But-3-enyl-(2,4-dimethoxy-benzyl)-carbamoyl]-pent-4-enoic Acid Methyl Ester (17). The same procedures as the general procedures for **7a** are followed. But-3-enyl-(2,4-dimethoxy-benzyl)-amine (500 mg, 2.26 mmol) was used and **17** (640 mg, 78%, oil) was obtained by flash chromatography (ethyl acetate/hexanes, 1/1). ^{1}H NMR ($CDCl_3$) δ 6.96 (d, J = 7.6 Hz, 1H), 6.44−6.42 (m, 2H), 5.72 (t, J = 8.3 Hz, 1H,), 5.12−4.97 (m, 4H), 4.47 (s, 2H), 3.76 (s, 6H), 3.63 (s, 3H), 3.33 (br t, 1H), 2.62−2.51 (m, 4H), 2.26 (q, J = 6.8 Hz, 2H); ESI (m/z) 384.5 (MNa^+).

3-[1-(2,4-Dimethoxy-benzyl)-2-oxo-1,2,5,6-tetrahydro-pyridin-3-yl]-propionic Acid Methyl Ester (18). The same procedures as the general procedures for **10a** are followed. Compound **17** (640 mg, 1.77 mmol) was used and **18** (580 mg, 98%, oil) was obtained by flash chromatography (ethyl acetate/hexanes, 1/1). ^{1}H NMR ($CDCl_3$) δ 7.19 (d, J = 3.0 Hz, 1H), 6.45−6.91 (m, 2H), 6.27 (t, J = 4.3 Hz, 1H), 4.55 (s, 2H), 3.78 (s, 6H), 3.63 (s, 3H), 3.30 (t, J = 7.1 Hz, 2H,), 2.63−2.50 (m, 4H), 2.23 (d, J = 6.7 Hz, 2H), 1.57 (s, 2H); ^{13}C NMR ($CDCl_3$) δ 173.6, 164.8, 160.2, 158.5, 134.2, 133.9, 130.4, 118.0, 104.1, 98.3, 55.2, 51.3, 45.0, 44.3, 33.3, 26.6, 23.9; ESI (m/z) 356.5 (MNa^+).

3-(2-Oxo-1,2,5,6-tetrahydro-pyridin-3-yl)-propionic Acid Methyl Ester (19). Compound **18** (490 mg, 1.47 mmol) was dissolved in 3 mL of TFA and then triethylsilane was added. The reaction

mixture was refluxed for 20 min at 8 °C. The solvent was removed in vacuo, and the residue was diluted in chloroform (50 mL). The organic layer was washed with satd $NaHCO_3$ solution (10 mL) and brine (10 mL). The organic layer was dried over anhydrous $MgSO_4$. Compound **19** (200 mg, 74%, solid) was obtained by flash chromatography (ethyl acetate/hexanes, 1/1). ^{1}H NMR ($CDCl_3$) δ 6.45 (s, 1H), 6.36 (t, J = 4.2 Hz, 2H), 3.61 (s, 3H), 3.31 (dt, J = 7.5 Hz, 2H), 2.55−2.45 (m, 4H), 2.27 (dd, J = 6.7, 5.8 Hz, 2H); ^{13}C NMR ($CDCl_3$) δ 173.41, 166.82, 136.09, 133.48, 51.35, 39.52, 33.06, 26.02, 24.01; ESI (m/z) 220.4 (MNa^+).

3-(1-Methyl-2-oxo-1,2,5,6-tetrahydro-pyridin-3-yl)-propionic Acid Methyl Ester (20a). To a solution of **19** (100 mg, 0.55 mmol) in THF (1.1 mL) was added NaHMDS (0.66 mL, 1.0 M in THF, 1.2 equiv) dropwise at −78 °C. After stirring at −78 °C for 30 min, dimethyl sulfate was added dropwise. The reaction mixture was stirred at −78 °C for 15 min and at 0 °C for 2 h. The reaction was quenched by satd NH_4Cl solution. The organic layer was extracted by ethyl acetate (30 mL × 3), and the combined organic layer was washed with satd NH_4Cl solution (10 mL) and brine (10 mL) and dried over anhydrous $MgSO_4$. Compound **20a** (80 mg, 74%, oil) was obtained by flash chromatography (ethyl acetate/hexanes, 1/1). ^{1}H NMR ($CDCl_3$) δ 6.28 (t, J = 4.2 Hz, 1H), 3.62 (s, 3H), 3.33 (t, J = 7.2 Hz, 2H), 2.96 (d, J = 3.2 Hz, 3H), 2.58−2.47 (m, 4H), 2.33−2.27 (m, 2H); ^{13}C NMR ($CDCl_3$) δ 173.90, 165.53, 134.33, 134.20, 51.65, 47.80, 34.86, 33.53, 26.80, 23.93; ESI (m/z) 220.4 (MNa^+).

General Procedures for 21a−c. *N*-Hydroxy-3-(1-methyl-2-oxo-1,2,5,6-tetrahydro-pyridin-3-yl)-propionamide (21a). The same procedures are followed as for **13a**. Compound **20a** (40 mg, 0.20 mmol) was used and **21a** (13.8 mg, 35%, oil) was obtained by flash chromatography (methanol/chloroform, 1/19). ^{1}H NMR ($CDCl_3$) δ 6.15 (t, J = 4.3 Hz, 1H), 3.41 (t, J = 7.2 Hz, 2H), 2.97 (s, 3H), 2.51 (t, J = 7.5 Hz, 2H), 2.35 (m, 2H), 2.22 (t, J = 7.5 Hz, 2H); ^{13}C NMR ($CDCl_3$) δ 170.56, 136.03, 47.72, 34.77, 31.68, 27.43, 23.61; ESI (m/z) 180.3 ($M^+ - H_2O$); HRMS (m/z; MH^+) calcd for $C_9H_{15}N_2O_3$, 199.1077; found, 199.1075.

3-(1-Allyl-2-oxo-1,2,5,6-tetrahydro-pyridin-3-yl)-*N*-hydroxy-propionamide (21b). The same procedures are followed as for **13a**. Compound **20b** (44 mg, 0.20 mmol) was used and **21b** (20 mg, 45%, oil) was obtained by flash chromatography (methanol/chloroform, 1/19). ^{1}H NMR ($CDCl_3$) δ 10.08 (br s, 1H), 8.76 (br s, 1H), 6.38 (br t, 1H), 5.75−5.67 (m, 1H), 5.17 (d, J = 5.4 Hz, 1H), 5.12 (s, 1H), 3.98 (d, J = 5.4 Hz, 2H), 3.30 (t, J = 7.0 Hz, 2H), 2.54 (s, 2H), 2.36−2.28 (m, 4H); ^{13}C NMR ($CDCl_3$) δ 170.17, 165.21, 136.15, 133.46, 132.91, 117.38, 49.25, 44.77, 32.72, 27.12, 23.74; ESI (m/z) 247.4 (MNa^+); HRMS (m/z; MH^+) calcd for $C_{11}H_{17}N_2O_3$, 225.1234; found, 225.1232.

3-[1-(2,4-Dimethoxy-benzyl)-2-oxo-1,2,5,6-tetrahydro-pyridin-3-yl]-*N*-hydroxy-propionamide (21c). The same procedures are followed as for **13a**. Compound **18** (46 mg, 0.14 mmol) was used and **21c** (32 mg, 73%, oil) was obtained by flash chromatography (methanol/chloroform, 1/19). ^{1}H NMR ($CDCl_3$) δ 7.12 (d, J = 9.0 Hz, 1H), 6.425−6.33 (m, 3H), 4.51 (s, 2H), 3.75 (s, 3H), 3.74 (s, 3H), 3.27 (t, J = 6.9 Hz, 2H), 2.55 (m, 2H), 2.38 (m, 2H), 2.22 (m, 2H); ^{13}C NMR ($CDCl_3$) δ 170.1, 165.4, 160.2, 158.5, 135.8, 133.5, 130.4, 117.5, 104.2, 98.3, 55.3, 44.9, 44.6, 32.8, 27.1, 23.8; ESI (m/z) 357.5 (MNa^+); HRMS (m/z; MH^+) calcd for $C_{17}H_{23}N_2O_5$, 335.1602; found, 335.1609.

Acknowledgment. This work was supported by a grant from KRIBB Research Initiative program and Grant 0405-NS01-0704-0001 of the Korean Health 21 R&D Project, Ministry of Health and Welfare, the Republic of Korea.

Supporting Information Available: Experimental procedures and characterization data of intermediates and final compounds, including biological procedures. This material is available free of charge via the Internet at http://pubs.acs.org.

References

(1) Balkwill, F.; Mantovani, A. Inflammation and cancer: Back to Virchow? *Lancet* **2001**, *357*, 539−545.

(2) (a) Castle, P. E.; Hillier, S. L.; Rabe, L. K.; Hildesheim, A.; Herrero, R.; Bratti, M. C.; Sherman, M. E.; Burk, R. D.; Rodriguez, A. C.; Alfaro, M.; Hutchinson, M. L.; Morales, J.; Schiffman, M. An association of cervical inflammation with high-grade cervical neoplasia in women infected with oncogenic human papillomavirus (HPV). *Cancer Epidemiol., Biomarkers Prev.* **2001**, *10*, 1021−1027. (b) Naumann, M.; Crabtree, J. Helicobacter pylori-induced epithelial cell signalling in gastric carcinogenesis. *Trends Microbiol.* **2002**, *12*, 29−36. (c) Rosin, M. P.; Anwar, W. A.; Ward, A. J. Inflammation, chromosomal instability, and cancer: The schistosomiasis model. *Cancer Res.* **1994**, *54(7)*, 1929S−1933S.

(3) Assenata, E.; Gerbal-chaloin, S.; Maurel, P.; José Vilarem, M.; Pascussi, J. M. Is nuclear factor kappa-B the missing link between inflammation, cancer and alteration in hepatic drug metabolism in patients with cancer? *Eur. J. Cancer* **2006**, *42*, 785−792.

(4) (a) Minucci, S.; Pelicci, P. G. Histone deacetylase inhibitors and the promise of epigenetic (and more) treatments for cancer. *Nat. Rev. Cancer* **2006**, *6*, 38−51. (b) Miller, T. A.; Witter, D. J.; Belvedere, S. Histone deacetylase inhibitors. *J. Med. Chem.* **2003**, *46*, 5097−5116.

(5) (a) Leoni, F.; Zaliani, A.; Bertolini, G.; Porro, G.; Pagani, P.; Pozzi, P.; Dona, G.; Fossati, G.; Sozzani, S.; Azam, T.; Bufler, P.; Fantuzzi, G.; Goncharov, I.; Kim, S.-H.; Pomerantz, B. J.; Reznikov, L. L.; Siegmund, B.; Dinarello, C. A.; Mascagni, P. The antitumor histone deacetylase inhibitor suberoylanilide hydroxamic acid exhibits antiinflammatory properties via suppression of cytokines. *Proc. Natl. Acad. Sci. U.S.A.* **2002**, *99*, 2995−3000. (b) Mishra, N.; Reilly, C. M.; Brown, D. R.; Ruiz, P.; Gilkeson, G. S. Histone deacetylase inhibitors modulate renal disease in the MRL-lpr/lpr mouse. *J. Clin. Invest.* **2003**, *111*, 539−552.

(6) Kim, H. M.; Lee, K.; Park, B. W.; Ryu, D. K.; Kim, K.; Lee, C. W.; Park, S.-K.; Han, J. W.; Lee, H. Y.; Lee, H. Y.; Han, G. Synthesis, enzymatic inhibition, and cancer cell growth inhibition of novel delta-lactam-based histone deacetylase (HDAC) inhibitors. *Bioorg. Med. Chem. Lett.* **2006**, *16*, 4068−4070.

(7) Finnin, M. S.; Donigian, J. R.; Cohen, A.; Richon, V. M.; Rifkind, R. A.; Marks, P. A.; Breslow, R.; Pavletich, N. P. Structures of a histone deacetylase homologue bound to the TSA and SAHA inhibitors. *Nature* **1999**, *401*, 188−193.

(8) (a) Papazisis, K. T.; Geromichalos, G. D.; Dimitriadis, K. A.; Kortsaris, A. H. Optimization of the sulforhodamine B colorimetric assay. *J. Immunol. Methods* **1997**, *208*, 151−158. (b) Skehan, P.; Storeng, R.; Scudiero, D.; Monks, A.; McMahon, J.; Vistica, D.; Warren, J. T.; Bokesch, H.; Kenney, S.; Boyd, M. R. New colorimetric cytotoxicity assay for anticancer-drug screening. *J. Natl. Cancer Inst.* **1990**, *82*, 107−1112.

(9) Hagler, A. T.; Lifson, S.; Dauber, P. Consistent force field studies of intermolecular forces in hydrogen-bonded crystals. 2. A benchmark for the objective comparison of alternative force fields *J. Am. Chem. Soc.* **1979**, *101*, 5122−5130.

(10) (a) The computational complex model was solvated using a solvent sphere of water extending 23.0 Å around the zinc ion, and only residues within 5.0 Å of compound **14d** were allowed to move during the geometry optimizations using 500 steps of steepest decent and 3000 steps of conjugated gradient. The hydroxamic acid coordinates of **14d** were restrained using 10.0 kcal/mol harmonic forces, the zinc ion VDW radius was taken from the work of Stote and Karplus. (b) Stote, R. H.; Karplus, M. Zinc binding in proteins and solution: a simple but accurate nonbonded representation *Proteins: Struct., Funct., and Genet.* **1995**, *23*, 12−31.

JM0613828